Organic Process Research & Development

Article

pubs.acs.org/OPRD

# Design of an Integrated Process of Chromatography, Crystallization and Racemization for the Resolution of 2′,6′-Pipecoloxylidide (PPX)

Jan von Langermann,[†] Malte Kaspereit,[‡] Mozaffar Shakeri,[§] Heike Lorenz,[†] Martin Hedberg,[⊥] Matthew J. Jones,[⊥] Kerstin Larson,[⊥] Björn Herschend,[⊥] Robert Arnell,[⊥] Erik Temmel,[†] Jan-Erling Bäckvall,[§] Achim Kienle,[∥,¶] and Andreas Seidel-Morgenstern*[,†,□]

[†]Max Planck Institute for Dynamics of Complex Technical Systems, Physical-Chemical Foundations of Process Engineering, Sandtorstraße 1, 39106 Magdeburg, Germany

[‡]Friedrich-Alexander University Erlangen-Nuremberg, Department for Separation Science and Technology, Egerlandstraße 3, 91058 Erlangen, Germany

[§]Department of Organic Chemistry, Arrhenius Laboratory, Stockholm University, 106 91 Stockholm, Sweden

[⊥]AstraZeneca AB, Pharmaceutical Development, Medicines Development, 151 85 Södertälje, Sweden

[∥]Max Planck Institute for Dynamics of Complex Technical Systems, Process Synthesis and Process Dynamics, Sandtorstraße 1, 39106 Magdeburg, Germany

Otto-von-Guericke University Magdeburg, [¶]Chair of Automation/Modeling and [□]Chair of Chemical and Process Engineering, Universitätsplatz 2, 39106 Magdeburg, Germany

**ABSTRACT:** An integrated process for the chiral separation of the industrially relevant substance 2′,6′-pipecoloxylidide (PPX), an intermediate in the manufacture of a number of anesthetics, was developed. By combining three different techniques, chromatography, crystallization, and racemization, high productivity was achieved. All unit operations were executed using a common solvent system, full recycling, and a minimum of solvent exchanges or removals. The target molecule was obtained with an enantiopurity of >99.5 wt %.

## 1. INTRODUCTION

**1.1. Potential Improvements in the Manufacture of (*S*)-2,6-Pipecoloxylidide.** 2′,6′-Pipecoloxylidide **1** (PPX) and its derivatives **2**–**4** (Figure 1) were first prepared and tested as local anesthetics in 1957[1] and **1** was found to be a useful intermediate for the synthesis of the commercial drugs mepivacaine **2**, ropivacaine **3**, and bupivacaine **4**. For example, bupivacaine is commonly used in its racemic form as an anesthetic during childbirth due to its long-lasting effect. Unfortunately, there are known toxicities associated with this drug. However, the pure (*S*)-enantiomer of **3** has a lower systemic toxicity than racemic bupivacaine, and the wider safety margin of (*S*)-**3** allows the use of higher concentrations and doses compared to that for bupivacaine, resulting in a lower risk of systemic toxicity and ensuring better surgical anesthesia.[2]

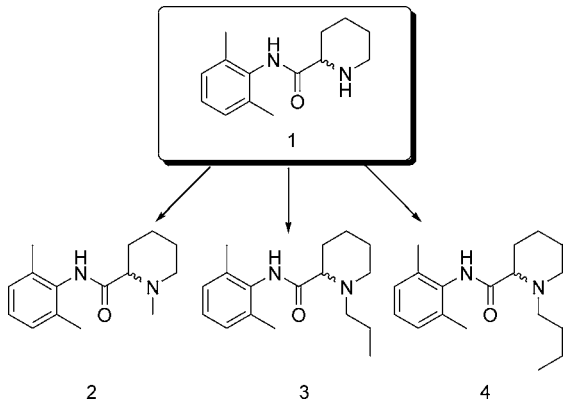


**Figure 1.** Structures of 2′,6′-pipecoloxylidide **1** and its derivatives mepivacaine **2**, ropivacaine **3**, and bupivacaine **4**.

On an industrial scale, racemic **1** is prepared either from racemic pipecolinic acid or via hydrogenation of 2′,6′-picolinoxylidide.[3] The (*S*)-enantiomer is then obtained via diastereomeric salt resolution using *O*,*O*-dibenzoyl-L-tartaric acid leaving the (*R*)-enantiomer as waste.[4] A further option is chiral pool synthesis from L-lysine, which has been reported to give (*S*)-**1** in a reasonable, 38% overall yield from CBz-mono-protected L-lysine.[3a] The latter route could perhaps become competitive after further optimization with an approach using resolution, but the apparently much more expensive[5] mono-CBz-protected analogue of L-lysine has been reported to be available through a two-step procedure from L-lysine at no more than 50–55% overall yield.[6] This results in an overall yield of the route from L-lysine to (*S*)-**1** of around 19% over six synthetic steps.

Furthermore, there are a number of different methods for making enantiomerically pure (*S*)-pipecolinic acid published in the literature,[7] and this is certainly a useful starting material for making compound (*S*)-**1**.[8] However, the cost of (*S*)-pipecolinic acid[5] is unfavorable when compared to that of the available

**Special Issue:** INTENANT

**Received:** September 30, 2011
**Published:** January 20, 2012

  

alternatives. Consequently, the shorter and more high-yielding[3c,d] resolution-based routes are currently more attractive from an economic perspective. The current AstraZeneca internal process design utilizes a diastereomeric salt resolution without recovery of the distomer. It is therefore of interest to investigate whether the process can be improved by integration of unit operations by coupling chromatography, enantioselective crystallization, and racemization for the recovery of the distomer in accordance with the INTENANT-concept.[9] The outcome of this study is described in this article. The knowledge gained from using **1** as a case study within INTENANT is also of general value for future products within the AstraZeneca development portfolio.

**1.2. Coupling of Chromatography, Crystallization, and Racemization.** Given the need to produce enantiopure (*S*)-PPX, all available separation strategies were compared with the aim of designing an efficient, fully integrated separation process. The main goal was to identify an improved process employing a combination of different unit operations while optimizing yield, productivity, and enantiopurity. Preliminary work within the INTENANT project revealed early on that a combination of chromatography, crystallization and racemization is a suitable approach. Further details are given in the paper by Kaspereit et al. in this issue of *Organic Process Research & Development*.[10]

Nonetheless, the combination of these different unit operations for the separation of PPX is challenging, since the individual operations require operating conditions that are not easily coupled. One critical issue identified early in the development is the need for a common solvent system capable of linking the individual unit operations (Figure 2) while reducing

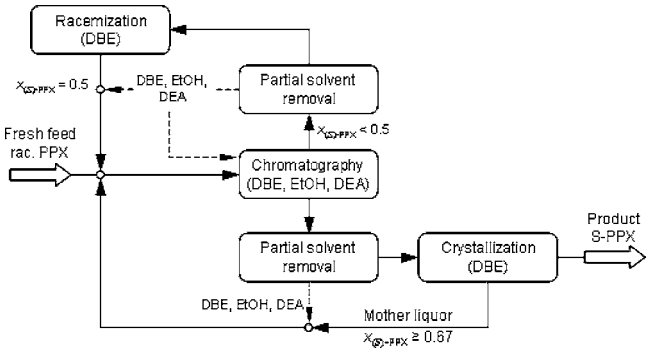


**Figure 2.** Integrated resolution process for PPX. Initially the racemic feed is enriched by chromatography. The resulting (*S*)-PPX-rich stream is then subjected to crystallization after which the mother liquor is returned to the chromatographic enrichment. The (*R*)-PPX-rich stream is racemized and then returned to the chromatographic separation. The primary function of the intermediate distillations is to adjust the composition of the solutions.

the need for solvent swaps or intermediate separations. This also included the consideration of secondary factors: preferably low toxicity of all substances involved, low cost and easy workup in the downstream processes. A manageable, low process complexity is also favored to ensure the practicability under industrial manufacturing conditions. Based upon these considerations, dibutylether (DBE) was chosen as the most suitable solvent, as it meets all the requirements mentioned above. The selection criteria included a suitable solubility of PPX for the final enantioselective crystallization, which is discussed below (see section 3.3) in addition to good compatibility with the other unit operations (see sections 2 and 4). Furthermore, the boiling point of DBE is significantly higher than that of any of the other components in the eluent system, ensuring good separability both within and outwith the integrated process.

Within this process, preparative chromatography employing an eluent system containing DBE, ethanol, and diethylamine (DEA) provides an enantioenriched solution, which is concentrated via distillation. The concentration step also serves to remove ethanol and DEA from the solvent. The concentrated solution is transferred to the crystallization process where the solid, enantiopure product is obtained. The residual mother liquor from the crystallization is recycled into the chromatographic separation since it contains an excess of the desired (*S*)-PPX. Simultaneously the (*R*)-enantiomer-rich stream from the initial chromatographic separation is racemized and eventually recycled into the separation cycle. Racemization of PPX is achieved by a homogeneous catalytic reaction employing the Shvo catalyst.[27b] Since only simple concentration adjustments are required between the different operations, process control is straightforward. Fortunately, azeotropes are absent in the eluent system (dibutylether/ethanol/diethylamine), and purification of the spent solvent mixtures is therefore not critical. This is primarily of relevance for the (re)adjustment of the eluent system for the next chromatographic separation cycle.

The main advantage of the process is its simple concept requiring only standard laboratory equipment, thus keeping costs low. All solvents as well as the undesired (*R*)-PPX are almost fully recycled, resulting in high atom efficiency. The investigations of the individual unit operations (chromatography, crystallization and racemization) within the common solvent system are described and discussed in the following sections (2 − 4). The results are evaluated and summarized with respect to their usability for an integrated resolution process for PPX.

## 2. CHROMATOGRAPHY

**2.1. Choice of Chromatographic System.** The choice of the stationary phase and the mobile phase is decisive for the performance of a chromatographic separation. Generally, the aim is to have high resolution, sufficient solubility, and low retention times. A significant number of chiral stationary phases (CSPs) and solvents were screened by pulse experiments on a 250 mm × 4.6 mm column packed with preparative CSPs with 20 $\mu$m particle size, and 'Chiralpak IC' was identified as the most suitable CSP for PPX.

With respect to the process concept in Figure 2, the mobile phase selected should also be compatible with the individual unit operations. A 85/15/0.1 (v/v/v) DBE/ethanol/diethylamine mixture was chosen as chromatographic solvent (separation factor $\alpha$ = 1.42). Ethanol and diethylamine volumes were selected to optimize retention times while ensuring sufficient separation efficiency. Beyond 85% of DBE the separation efficiency increases only slightly, but retention times rise significantly. The high boiling point of DBE together with the absence of azeotropes ensures efficient removal of ethanol and DEA in the subsequent solvent evaporation.

Despite the high separation factor, full baseline separation was unfortunately never observed. This is due to a peculiar adsorption behavior, which will be discussed in more detail below. However, in view of the combined process this is less relevant, since chromatography is required to perform only a partial separation and enrichment. In fact, the combination of


dx.doi.org/10.1021/op200268h | *Org. ProcessRes. Dev.* 2012, 16, 343−352

chromatography and crystallization[11−13] required by the scheme in Figure 2 is particularly useful in cases where chromatographic performance is limited.

**2.2. Column Model.** The chromatographic separation step was designed on the basis of a mathematical column model. Here the transport-equilibrium model is applied, which consists of the following component mass balances

$$\frac{\partial c_i}{\partial t} + \frac{1-\varepsilon}{\varepsilon}\frac{\partial q_i}{\partial t} + u\frac{\partial c_i}{\partial z} = D_{ax}\frac{\partial^2 c_i}{\partial z^2} \quad (1a)$$

$$\frac{\partial q_i}{\partial t} = k_{f,i}[q^*_i(\bar{c}) - q_i],\ i = (1, 2) \quad (1b)$$

In these equations, $c_i$ and $q_i$ are the concentrations of component $i$ in the fluid and the loadings on the CSP, respectively. The competitive adsorption equilibrium is denoted by $q^*_i(\bar{c})$; $\varepsilon$ is the bed porosity, $u = Q/(\varepsilon A)$ is the interstitial fluid velocity, $Q$ the volumetric flow rate, and $D_{ax}$ the axial dispersion coefficient. Equation 1b describes mass transfer between the two phases by a solid film driving-force approach.

The model equations were implemented in Matlab and solved by an explicit backward−forward finite difference scheme that approximates the axial dispersion term in eq 1a numerically (see refs 14 and 15 for details).

**2.3. Parameter Determination.** Before applying the above column model the unknown parameters in eqs 1a and 1b have to be determined experimentally. Table 1 lists the parameter values obtained from simple injections of small pulses at dilute conditions at 25 °C.

**Table 1. Determination of model parameters for eqs 1a and 1b[a]**

| parameter | value | determination procedure |
|---|---|---|
| $Q$ [mL/min] | 2 | chosen as compromise between efficiency and throughput |
| $\varepsilon$ | 0.706 | retention time $t_0 = \varepsilon V/Q$ of nonadsorbing DBE |
| $K_i$ | 7.52 | from retention times $t_{R,i}$ of small racemate injections, using |
| | 10.25 | $t_{R,i} = t_0[1+(1-\varepsilon)/\varepsilon\ K_i]$ |
| $N_{app,i}$ | 160 | from small racemate injections, using $N_i \approx 5.54 t^2_{R,i}/w^2_{50}$, with $w_{50}$ as peak |
| | 185 | width at half its height |
| $D_{ax}$[m$^2$/s] | $2.84 \times 10^{-7}$ | Chung and Wen correlation,[16] value corresponds to $N_{ax} = uL/(2\ D_{ax})$=1250 |
| $k_{f,i}$[1/s] | 1.043 | from eq 2 for $D_{ax} = 2.84 \times 10^{-7}$ m$^2$/s |
| | 0.686 | |
| $D^{sim}_{ax}$[m$^2$/s] | $7.10 \times 10^{-7}$ | corresponds to $N_{ax} = 500$ (chosen for simulation) |
| $k^{sim}_{f,i}$[1/s] | 1.485 | from eq 2 for $N_{ax} = 500$ |
| | 0.895 | |

[a]The index $i = (R, S)$ denotes the two enantiomers, where $S$ is weaker adsorbing.

Standard methods are used for determination of the parameters given in Table 1. Merely the determination of the mass transfer coefficients, $k_{f,i}$, requires further explanation. These were calculated from the measured apparent stage numbers, $N_{app,i}$, the axial dispersion coefficient, $D_{ax}$, and the retention factors, $k'_i$, using the equation reported by Guiochon et al.[17]

$$H_i(u) = \frac{L}{N_{app,i}} = \frac{2D_{ax}}{u} + 2\left(\frac{k'_i}{1+k'_i}\right)^2 \frac{u}{k'_i k_{f,i}} \quad (2)$$

Concerning the spatial discretization of the eqs 1, the stage number $N_{ax} = 1250$ corresponding to the $D_{ax}$ predicted from the correlation by Chung and Wen[16] leads to unacceptably high computation times. Therefore a lower value of $N^{sim}_{ax} = 500$ was chosen for these simulations. The corresponding coefficients $k^{sim}_{f,i}$ were recalculated from eq 2. This speeds up calculations by a factor of 4 without observable loss of predictive quality.

Competitive adsorption isotherms $q^*_i(\bar{c})$ were determined by the inverse method, see for example ref 18. In this method, which was applied simultaneously to 12 different experimental chromatograms, the differences between simulated and experimental elution profiles are minimized using an optimizer (here: fminsearch in Matlab) that adjusts the isotherm parameters.

As mentioned earlier, initial experiments indicated a partially collaborative adsorption. Thus, several different isotherm models were investigated. A sufficiently accurate description was achieved using the following expressions:

$$q_i = \gamma \cdot c_i + q^I_s \frac{b^I_i}{1+\sum_j b^I_j c_j} + q^{II}_s \frac{b^{II}_i c_i + 2b_{q,i}c_i^2 + b_m c_R c_S}{1+\sum_k b^{II}_k c_k + \sum_n b_{q,n}c_n^2 + b_m c_R c_S},$$
$$i = (R, S);\ j, k, n = R...S \quad (3)$$

This isotherm model implies a simultaneous linear ($\gamma$), Langmuir-type (I) and competitive−collaborative (II) adsorption behaviors. The number of free parameters was reduced to 8 by requiring that the initial slopes correspond to the measured values in Table 1, i.e. $q^*_i(\bar{c}\to 0) = K_i$. The parameters are valid in the investigated concentration range up to 70 g/L (rac.), specifically: $\gamma = 0.6331$, $q^I_s = 64.7$ g/L, $b^I_S = 0.0316$ L/g, $b^I_R = 0$, $q^{II}_s = 46.8$ g/L, $b^{II}_S = 0.1035$ L/g, $b^{II}_R = 0.2056$ L/g, $b_{q,S} = 0.0056$ L$^2$/g$^2$, $b_{q,R} = 0.0258$ L$^2$/g$^2$, and $b_m = 0.0188$ L$^2$/g$^2$.

The model was validated by simulating independent experiments. Figure 3 shows two decisive examples where asymmetric mixtures were injected. The agreement between experiment and model prediction is very good.

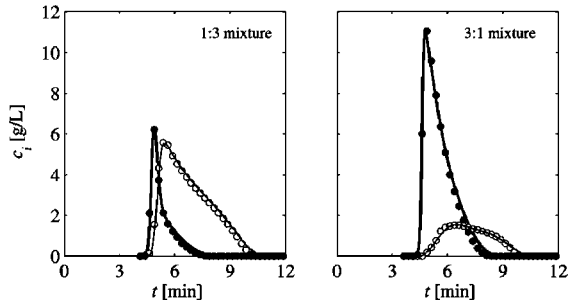


**Figure 3.** Validation of the model (lines) against independent experiments (symbols) with asymmetric injection compositions. (Left) Injection of a 1:3 ($S$:$R$) mixture. (Right) Injection of a 3:1 ($S$:$R$) mixture. Injection volume 2 mL, total injection concentration 20 g/L.

**2.4. Steady-State Recycling Chromatography.** Chromatographic separation was performed by a specific operating mode known as steady-state recycling (SSR).[19,20] In this process a large injection is applied, which results in only partially resolved elution profiles. The sufficiently purified leading and trailing edges of the profile are collected as product fractions. A constant amount of fresh feed is added to the remaining


dx.doi.org/10.1021/op200268h | Org. ProcessRes. Dev. 2012, 16, 343−352

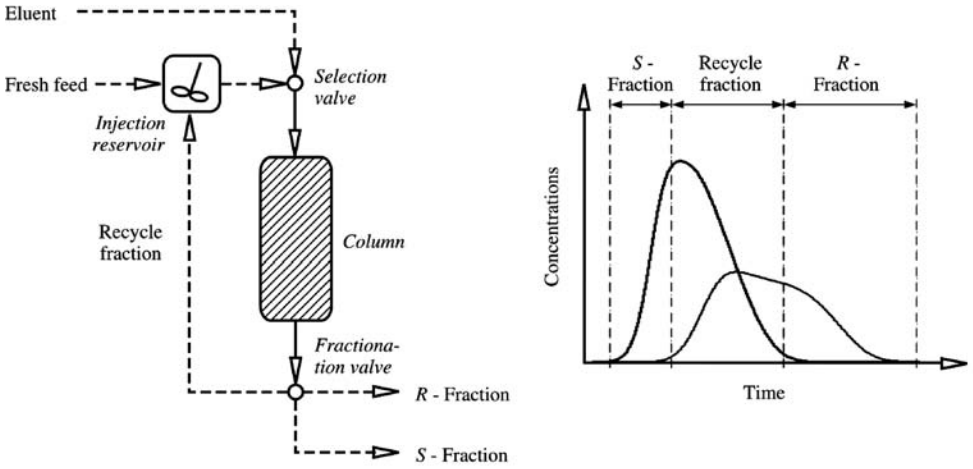


**Figure 4.** Schematic setup of SSR chromatography (left) with elution profiles and cut times in the steady state (right). Here, recycle and fresh feed are mixed (mixed recycle mode, MR-SSR).[19] For this mode shortcut design methods are available.[21,22] Alternatively, the mixed fraction can be recycled directly to the column (closed-loop mode, CL-SSR).[20]

unresolved part and then reinjected. After several cycles, a periodic steady state is attained. The principle is illustrated in Figure 4.

Under preparative conditions a properly designed SSR process can achieve significantly higher productivity, higher product concentrations, and lower eluent consumption than batch chromatography at the same purity and yield.[21]

The main design parameters for SSR chromatography are the four cut times (cf. Figure 4) that define the product fractions and the injection volume. Two shortcut design methods are available[21,22] that allow a simple determination of the cut times for any purity requirements. Here the method proposed by Kaspereit and Sainio[21] is applied, requiring only a simple evaluation of single chromatograms, and a rapid design study was performed by taking the required "input chromatograms" from simulations. It was found that, due to the specific adsorption behavior of PPX, performance improves particularly well when decreasing the purity requirement from the pure enantiomer to lower values. Due to this behavior the injection concentration should also be optimized. A rough estimation indicated that a purity of 95% for both fractions and a fresh feed concentration of 25 g/L (racemic mixture) represent useful conditions for the coupled process. Figure 5 shows the performance of the SSR process as a function of the injection volume. It can be seen that the SSR process (small symbols) clearly outperforms conventional batch chromatography (large symbols). The optimum injection volume for SSR is approximately 2.5 mL.

The above procedure was applied to design several experimental SSR runs for different purity requirements and different start-up conditions. In all cases very good agreement between the experimental results and design specifications was achieved. As an example, Figure 6 shows the results for the optimum injection volume of 2.5 mL and the desired purity of 95%. In this example, the transient start-up period of the process was essentially eliminated by using the steady-state injection concentrations predicted by the model for the first two injections (see refs 21 and 22 for details on this approach). Steady-state is readily obtained after about three cycles. Elution profiles, collected fraction concentrations, and purities (symbols) are very close to the simulation results.

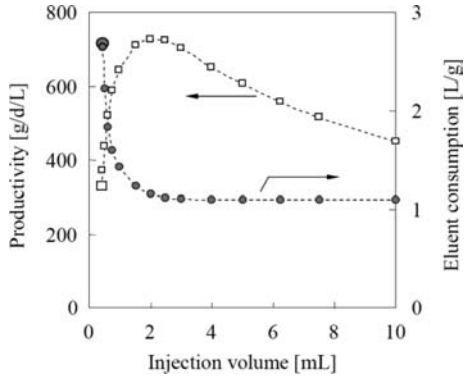


**Figure 5.** Optimized performance of the MR-SSR process as function of the injection volume for a fresh feed concentration of 25 g/L (rac.). Open symbols - productivity (product amount per time and volume of stationary phase). Filled symbols - solvent requirement (solvent amount per product amount). Large symbols at the left mark the optimized batch chromatography process that achieves the same yield (i.e., so-called touching band conditions, no waste fraction).

Note that a further performance improvement is possible by choosing the first cut time closer to the first product peak. In the current case this would result in a temporal overlap of recycling and injection, which is not accounted for in the shortcut design method. If the resulting slight purity deviations cannot be accepted, this can be dealt with by using the model to fine-tune the cut times, or by temporarily storing the recycle fraction and reinjecting it in the next-but-one cycle (as was assumed for Figure 6). Since the purpose of the experiments performed was to assess process feasibility, such overlap was prevented by applying safety margins between the injections.

In summary, a highly efficient chromatographic system was found, which was executed under reduced purity requirements. A full separation of PPX was neither possible nor necessary, since the enantioenriched solution was transferred to a crystallization process yielding the enantiopure product. See Kaspereit et al. within this issue of *Organic Process Research & Development* for further details.[10]


dx.doi.org/10.1021/op200268h | *Org. ProcessRes. Dev.* 2012, 16, 343–352

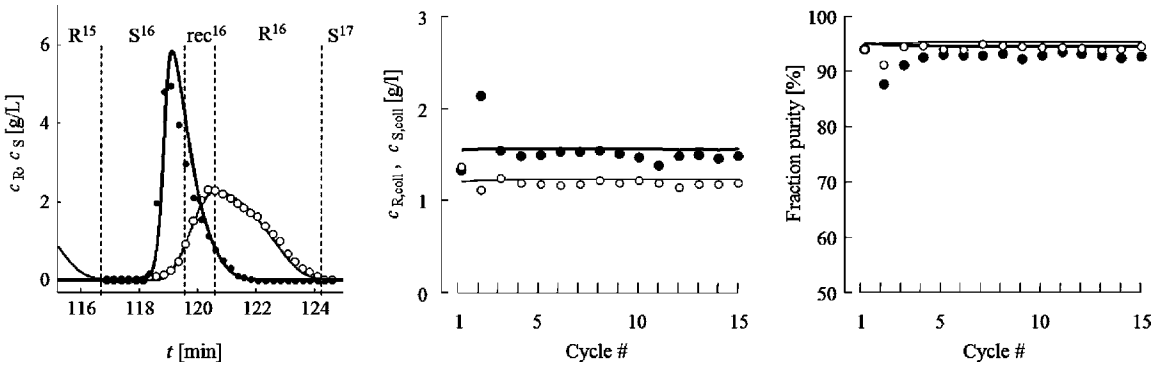


**Figure 6.** Results of an SSR experiment with 16 cycles. Sampled elution profiles of the final cycle (left), concentrations in collected fractions (middle), and fraction purities (right) in comparison to model predictions. Symbols - experimental results. Lines - simulation results. Filled symbols/thick lines mark the (*S*)-enantiomer (the first fraction); open symbols/thin lines mark the (*R*)-enantiomer (second fraction). Experimental conditions: fresh feed 25 g/L (rac.); injection volume 2.52 mL; flow rate 2 mL/min; cut times 3.45, 6.29, 7.35, 11.0 min. Injections performed every 7.55 min (corresponds to the cycle time of 11.0 − 3.45 min).

## 3. CRYSTALLIZATION

Previous crystallization process development and understanding was limited to the hydrochloride salt of PPX, which was obtained directly from synthesis and used for further processing. However, the protonated form of PPX is not suitable for use in the proposed integrated process, and therefore the final crystallization was redesigned for the neutral form. The characterization of the crystallization behavior of racemic as well as enantiopure PPX required for the design process revealed new opportunities for process solutions for manufacture of the single enantiomer.

**3.1. Physical/Chemical Properties of PPX: Solid Phase Behavior and Melt Phase Diagram.** The solid phase behavior of the neutral form of PPX defines the overall design of the integrated process, since the requirements of the crystallization process define the purity required from the preceding chromatographic enrichment.[23] Here, X-ray powder diffraction (XRPD) was used to characterize the phase behavior of PPX. As shown in Figure 7, the powder patterns of the racemate and the enantiomer are clearly distinct, indicating a racemic compound-forming system.

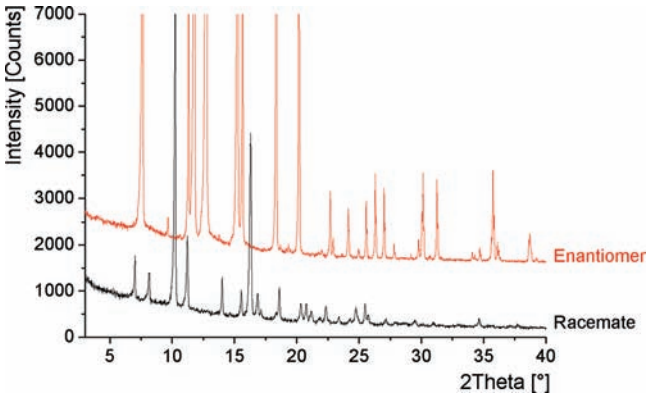


**Figure 7.** XRPD-patterns of PPX; racemate (black) and enantiomer (red), indicating a racemic compound-forming behavior.

The melting temperatures, the corresponding heats of fusion (Table 2), and the melt phase diagram (see Figure 8) support the interpretation of the diffraction patterns. The enantiomer melts at a higher temperature than the racemate, approximately 405 and 388 K respectively, while the heats of fusion are very similar. The values determined here compare favorably to those reported by Nemak et al.[25]

**Table 2. Melting temperatures and heats of fusion of the pure enantiomer and the racemic compound of PPX, both in their neutral forms**

| | melting temperatures - $T^f$ / K | | heat of fusion - $\Delta H^f$ / kJ·mol$^{-1}$ | |
|---|---|---|---|---|
| | own work | literature[25] | own work | literature[25] |
| enantiomer | 404.84 | 403.15 | 25.84 | 24.19 |
| racemate | 387.85 | 385.15 | 24.12 | 23.13 |

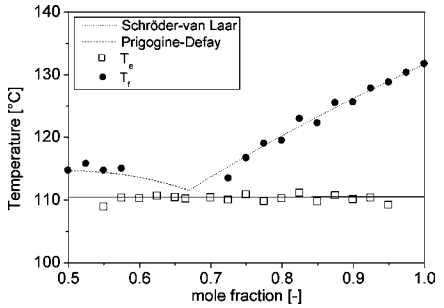


**Figure 8.** Binary melt phase diagram of PPX, neutral form; liquidus curves calculated using the Schröder-van Laar and Prigogine-Defay equations are indicated by dotted and dashed lines. The eutectic composition lies at $x(S)$-PPX = 0.67 (only one-half of the phase diagram is shown), $T_e$ - eutectic temperature, $T_f$ - temperature on the liquidus line.

As no decomposition or solid phase transitions were observed during the measurements on the pure enantiomer and the racemic compound, the binary phase diagram was determined. The system was found to behave almost ideally, the experimentally determined liquidus and solidus lines match the calculated Schröder-van Laar and Prigogine-Defay lines[23] (Figure 8), and the eutectic composition was found at a mole fraction of $x$ = 0.67. The eutectic composition is a critical factor in the integrated process design, as it represents the minimum enrichment required from the chromatographic step and the lower composition limit of the system for crystallization of the pure enantiomer. This specific position of the eutectic is favorable for a combination of enantioenrichment via chromatography and enantioselective crystallization, since only a moderate enrichment is required.[13,26]


dx.doi.org/10.1021/op200268h | Org. ProcessRes. Dev. 2012, 16, 343−352

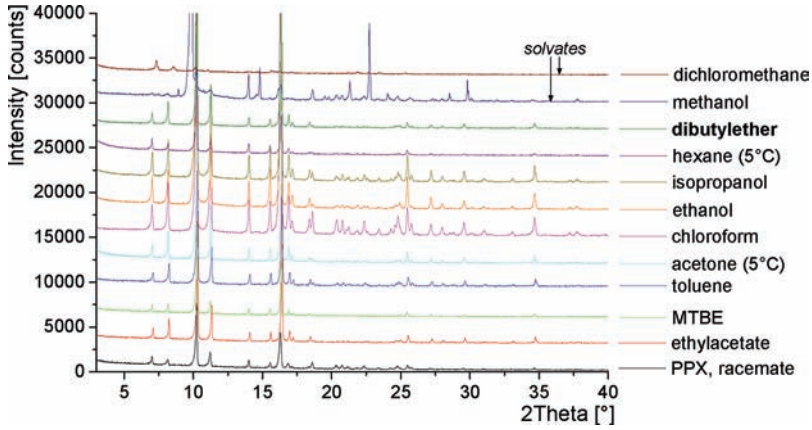


**Figure 9.** XRPD-screening for solvent-mediated polymorphism and solvate formation for racemic PPX. No polymorphs were identified and only two solvates (with dichloromethane and methanol at the top of the graph) were found. The results were verified by solution NMR (data not shown). No solvates were found for the pure PPX-enantiomer.

As seen in the phase diagram (Figure 8) and also verified by a Tammann plot (data not shown), the PPX-system shows complete immiscibility in the solid state.

**3.2. Solvate and Polymorph Screening.** A polymorph and solvate screen was included early in the process development as part of the solvent screen and in order to identify potential problems with undesired crystal modifications.[23] The results from the screen are also of value to the chromatography and racemization process development as they ensure that the most suitable solvent for all operations can be identified. Here, dibutylether was identified as the most suitable solvent for all operations.

Only two solvates were found, a dichloromethane solvate and a methanol solvate. Consequently, these solvents were not considered in the further investigations. XRPD-patterns for the solid phases obtained in the screening process are shown in Figure 9.

While the solution−crystallization-based polymorph screen was negative, one polymorph of the racemic compound was identified via melt crystallization. This polymorph has a distinct XRPD pattern (Figure 10a) and is clearly metastable as it transforms back to the stable modification with a half-life of ~300 min (Figure 10a,b). Full thermal characterization is precluded by an increased transition rate at elevated temperatures. As this polymorph is a polymorph of the racemic compound and the target species here is the pure enantiomer, its existence is of no relevance to the process.

**3.3. Enantioselective Crystallization.** The ternary solubility phase diagram of PPX was determined in the selected process solvent, dibutylether. Solubility data were measured in the temperature range from 5 to 55 °C, and the solubilities of both the pure enantiomer and the racemic compound were shown to increase with temperature (Figure 11).

While the eutectic composition is independent of temperature, a subtle shift of the eutectic composition determined from the ternary phase diagram measurements to x = 0.7 compared to the composition of the eutectic from the binary phase diagram (x = 0.67) was observed. It is likely that this difference is simply due to experimental error and for the purpose of crystallization process development the solution value is used. Solid phase analysis confirmed that only the stable PPX modifications, as shown in Figure 7, were present.

Initial validation of the suggested separation route of SSR-chromatography and enantioselective crystallization was carried

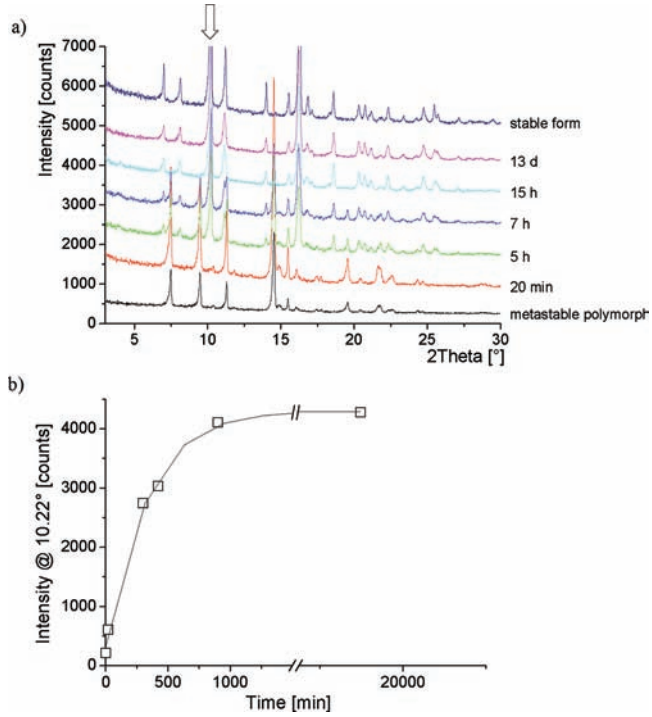


**Figure 10.** (a) Transition of the metastable polymorph of the racemic compound to the stable modification as followed by XRPD; (b) tracking of the intensity evolution for the peak at 10.2° (marked with an arrow in (a)), revealed a half-life of ~300 min for the metastable modification. The measurements were executed at ambient temperature.

out at the gram-scale at MPI-Magdeburg, later repeated at a larger scale employing several 100 g of PPX at AstraZeneca, Södertälje (results not shown here). The small scale experiment started with an enantioenriched solution of 93.4% (*S*)-PPX in the eluent system dibutylether/ethanol/diethylamine (DBE/EtOH/DEA), which was obtained from SSR-chromatography as described in section 2.4. The dilute, unsaturated solution from chromatography was concentrated by partial solvent evaporation, which removed all remaining ethanol and diethylamine and a fraction of the dibutylether. The concentrated solution was finally charged to the crystallization vessel and (*S*)-PPX was obtained with an enantiopurity of ≥99.5%, which fulfills the minimum requirement of 99.0%. The large-scale-validation at


dx.doi.org/10.1021/op200268h | *Org. ProcessRes. Dev.* 2012, 16, 343−352

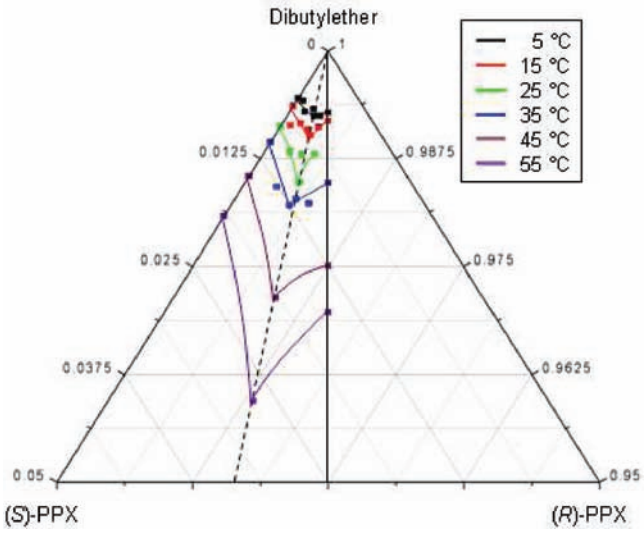


**Figure 11.** Ternary phase diagram of PPX in dibutylether. The solubility increases with temperature, and the eutectic composition is independent of temperature. Due to the advantageous position of the eutectic composition and the sufficiently strong temperature dependence of the solubility, enantioselective crystallization of enantiopure PPX is feasible by means of a simple cooling crystallization.

AstraZeneca confirmed the results from the small-scale experiments, underlining the general applicability of the integrated process. The mother liquor, depleted but still enriched with respect to (*S*)-PPX (≥70%), was recycled into the chromatographic separation after adjustment of the solvent to the specification of the eluent system (as shown in the general process scheme, Figure 2). During the entire crystallization process, no formation of byproduct, which may interfere with subsequent chromatography or racemization cycles, was observed.

In summary, the crystallization process facilitates the production of enantiopure PPX by crystallization from dibutylether. A sufficient enantiopurity of PPX was achieved and the remaining mother liquor was recycled to chromatography, ensuring an optimal separation process. Racemization of the undesired (*R*)-enantiomer is essential to raise the overall-yield of the PPX-separation process as without this operation the combination of chromatography and crystallization do not provide sufficient process improvement.

## 4. RACEMIZATION

Resolution processes starting from racemic mixtures are limited to a maximum yield of 50%, namely the eutomer fraction of the racemic mixture, while the distomer is merely waste. A racemization of the distomer is therefore highly desirable in order to recover the eutomer from the distomer stream and to increase the overall process yield and efficiency.

Within INTENANT, investigation of racemization techniques included several studies aimed at developing novel methodologies to racemise important structural classes such as amino acids and their derivatives, amines and alcohols. In case of PPX, prior state-of-the-art was to use stoichiometric amounts of sodium ethoxide[29] for racemization. Very long reaction times (>5 d) were required and several side reactions resulted in undesired impurities. Other studies demonstrated the successful use of metal catalysts[27] and heating in polar protic solvents.[28] In the course of the INTENANT work a novel homogeneous catalytic method for the racemization of (*R*)-PPX using Shvo's catalyst (Figure 12) was identified (ref.[27a−d] and below). (*S*)-PPX was used for the initial studies, since it was more easily available than its (*R*)-form.

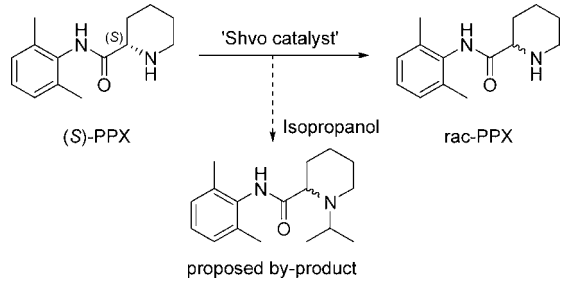


**Figure 12.** Reaction scheme for the PPX-racemization. Use of alcohols such as ethanol or isopropanol results in an undesired side reaction, which necessitates the removal of ethanol from the chromatography eluent prior to racemization.

Initial racemization experiments included isopropanol in the solvent in order to enhance the solubility of PPX, as the solubility in dibutylether is limited (section 3.3). The results of these studies are given in Table 3. Substoichiometric

**Table 3. Racemization of PPX in the presence of isopropanol[a]**

| entry | isopropanol (equiv.) | time (h) | ee (PPX) | byproduct |
|---|---|---|---|---|
| 1 | 0 | 1 | <1 | – |
| 2 | 0.5 | 1 | 2.4 | 0 |
| 3 | 1[b] | 1 | 1 | 0 |
| 4 | 10[c] | 1 | 22 | 4.5 |
| | | 2 | 1.1 | 9.4 |

[a]Reaction conditions: Shvo's catalyst (2 mol %), 0.5 mmol (*S*)-PPX, isopropanol (*x* equiv), dibutylether (2 mL), temp. 140 °C. [b]The presence of 1 equiv of isopropanol in the racemization mixture prolonged crystallization of PPX to over 12 h. [c]The presence of 10 equiv of isopropanol in the racemization mixture does not allow crystallization of PPX due to enhanced solubility.

(0.5 equiv) and stoichiometric addition of isopropanol to the reaction mixture did not affect the racemization rate (Table 3, compare entries 2 and 3 with entry 1) and no byproducts were observed. The stoichiometric addition of isopropanol to the racemization mixture resulted in an extended crystallization time of PPX from one hour to one night at room temperature. When (*S*)-PPX was racemized in the presence of 10 equivalents of isopropanol, the racemization rate decreased (Table 1, entry 4) and byproduct formation according to Figure 12, was observed.

Consequently the use of isopropanol was avoided during PPX-racemization since the corresponding impurities will eventually accumulate throughout the process. Accumulation within the recycled material is likely to have a detrimental effect upon both chromatography and crystallization.

A major advantage of the proposed separation process is the full recycling of (*R*)-PPX and all other chemicals used, including the repeated use of the racemization catalyst. Considering its cost, recycling of the catalyst is almost mandatory for an economically advantageous process. Furthermore, the racemization of highly concentrated PPX solutions is desirable at the manufacturing scale. Therefore the effect of catalyst recycling and high PPX concentrations was investigated and the results are summarized in Table 4.


dx.doi.org/10.1021/op200268h | *Org. ProcessRes. Dev.* 2012, 16, 343−352

**Table 4. Racemization of high concentrations of PPX and repeated use of mother liquor[a]**

| entry | batch no. | time (h) | ee (PPX) | yield[b] |
|---|---|---|---|---|
| 1 | 1 | 1 | 0 | 86 |
| 2[c] | 2 | 1 | 15 | 91 |
| 3[c] | 3 | 1 | 40 | 92 |
| 4[c] | 4 | 1 | 70 | ~100 |

[a]Reaction conditions: Shvo catalyst (1 mol %), (*S*)-PPX 1 mmol, $Bu_2O$ (2 mL), temp. 140 °C. [b]Yield = (mass of solids isolated after reaction)/ (initial mass of substrate − mass of substrate taken for sampling). [c]Volume of mother liquor removed by syringe after reaction was 1.6 mL. Thus, the crystals from the reaction were washed with a further 400 μL of $Bu_2O$ and were then transferred to the new racemization solution.

Racemization reactions employing higher concentrations (~10%, entry 1) and lower concentrations (~5%, entry 2) of (*S*)-PPX were completed in 1 h. With continuous recycling of the catalyst the catalytic efficiency decreases, while the enantiomeric excess obtained increases simultaneously from 0% (full racemization) to 15%, 40%, and 70%, respectively. This effect can be explained by a loss of Shvo's catalyst in the mother liquor by 10% based on sample volume in addition to deactivation of the catalyst during the racemization reactions. In solution, the catalyst is known to be sensitive to oxygen, the presence of which results in deactivation. It is worth mentioning that the reaction mixture gradually turned red from the first to the fourth batch of racemization. The loss of catalytic activity was significantly reduced at the large scale, possibly as a result of the reduced relative surface area of the solvent exposed to the atmosphere, thus reducing the effect of oxygen.

## 5. INTEGRATED PROCESS

Combining chromatography, crystallization and racemization into an integrated process provides for significant improvements compared to a single purification process. Table 5 comparing the original process with the individual unit operations and the combined process, highlights these improvements.

Starting with option one, the classical diastereomeric salt resolution as 'state of the art' was originally used to obtain the enantiopure product. The very easy setup and simple process control is tarnished by the limited maximum yield of 50% and high waste production. However, from an industrial point of view, this process was preferred for many years due to low cost.

Option two, chromatographic separation, is an interesting alternative, but full separation is precluded due to high cost and the large eluent volumes required. Costs, productivity, and solvent consumption can be reduced significantly if the purity requirements from chromatography can be relaxed (see ref 10), while the purity requirements for the product can then no longer be met. Enantioselective crystallization (option three) is not possible for a racemic compound-forming system when starting from a racemic mixture and requires prior enrichment to a composition above the eutectic. Clearly, options two and three lend themselves to coupling within an integrated process, where the gain in productivity and reduced solvent consumption of a chromatographic process with lower product purity requirements may outweigh the cost of an additional crystallization operation. For PPX, asymmetric synthesis (option four) is not viable for the simple reason that no effective process is known. As a consequence options 2 and 3 as well as a racemization reaction were developed as coupled processes, which successfully improved the overall process efficiency. Even though neither of the processes, taken in isolation, operates in an optimal manner, the combination of the three operations allows their disadvantages to be minimized while optimizing the entire process with respect to productivity, efficiency and yield. The proposed process was finally validated in lab- and large scale experiments.

On the basis of the encouraging results of the SSR chromatography experiments (section 2.4), the process was initially combined with a crystallization step. A longer production run was conducted in order to obtain a sufficient amount of a partially enriched solution that was then subjected to an enantioselective crystallization. The same operating parameters as those reported in Figure 6 were applied in an experiment with 126 cycles (16 h). This resulted in 775 mL of the first product fraction with a purity of 93.4% (design value 95%) with respect to the eutomer. The overall productivity is about 270 g $d^{-1}$ $L^{-1}$, which is lower than the predicted 730 g $d^{-1}$ $L^{-1}$ (Figure 5). The reduced productivity is due to the safety margins applied between the injections, as discussed above. From the solution collected, a total of 470 mg of solid (*S*)-enantiomer was crystallized in enantiomerically pure form, which corresponds to a yield of 54%. It must be noted that a rather conservative crystallization procedure was applied at this initial stage in order to keep a sufficient distance to the eutectic composition at 70% in solution. At this point racemization of the undesired enantiomer was not considered as the process described above was still under development. The full integrated process was validated at AstraZeneca, Södertälje, on a larger scale employing several 100 g of PPX. These experiments confirmed the validity of the general approach and its applicability to industrial processes.

## 6. CONCLUSION

A novel, integrated, chiral resolution process combining chromatography, crystallization, and racemization was investigated for 2′,6′-pipecoloxilidide (PPX). A significant improvement in process efficiency was obtained by the systematic coupling of these unit operations. Preparative chromatography was used to obtain an enantioenriched solution from the initial, racemic mixture of PPX. Despite the fact that the 'chromatographic separation' employed provides unsatisfactory resolution

**Table 5. Comparison of PPX-resolution strategies**

| option | type | advantage(s) | disadvantage(s) | feasibility for separation of PPX |
|---|---|---|---|---|
| 1 | classical resolution-*state of the art*- | simple process design | waste disposal, max. 50% yield | yes |
| 2 | chromatographic separation | purity freely adjustable | cost (for bulk production) | no |
| 3 | enantioselective crystallization | simple process design | enantioenrichment necessary | no |
| 4 | asymmetric synthesis | low waste generation | no process available | no |
| **5 (combination of 2 + 3 + racemization)** | **integrated process** | **high yield and productivity, waste reduction** | **complexity** | **yes** |


dx.doi.org/10.1021/op200268h | *Org. ProcessRes. Dev.* 2012, 16, 343–352

when assessed in isolation, the reduced purity requirements lead to improved productivity, reduced eluent volumes, and an output stream that is sufficiently enriched for enantioselective crystallization. An enantioselective crystallization is then used to isolate the pure (*S*)-PPX with a purity of ≥99.5%, while the remaining, enriched mother liquor is recycled into the chromatographic separation. The (*R*)-PPX-rich chromatography stream is racemized using a homogeneous catalyst, which yields a racemic mixture of PPX that is also recycled into the chromatography enrichment, together with fresh feed. The basis for the entire process is, on the one hand, the existence of a common solvent system that can be used in all three unit operations and, on the other hand, the operating conditions for the individual unit operations that minimize their disadvantages while improving the overall process.

## 7. EXPERIMENTAL SECTION

(rac)-PPX and (*S*)-PPX were provided by AstraZeneca both in their neutral forms and as hydrochloride salts. All other chemicals were obtained in analytical purity and were used without any further purification. For racemization studies dibutylether was dried over molecular sieves prior to use.

**Chromatographic Separation.** The eluent system consisted of a mixture of DBE/EtOH/DEA. 85/15/0.1 (v/v/v). A Chiralpak IC column from Chiral Technologies (West Chester/PA, U.S.A.) was used throughout the whole study. Temperature control of the column (at 25 °C) was provided by a Lauda Ecoline RE306 (Lauda, Germany) thermostat. A modular experimental setup was applied consisting of K-1001 HPLC pumps, UV detector Smartline 2500, and K-6 and K-17 valves for switching (injection, fractionation, and recycling) (all Knauer GmbH, Germany). The system was controlled via an RS232 interface and used a custom Labview program (Labview 7.0, National Instruments, U.S.A.). Injections in the SSR experiments were performed through an HPLC pump using a K-6 valve as selection valve.

HPLC analysis of collected samples was performed on an Agilent HP 1100 using a Chiralcel OD column (150 mm × 4.6 mm, 5 $\mu$m) with *n*-hexane/isopropanol/triflouroacetate (85/15/0,1 v/v) as solvent and a UV-detector.

**Solid-Phase Investigations and Solubility.** Differential scanning calorimetry (DSC) experiments were performed on a DSC131 from Setaram (France). The start temperature was 30 °C, the final temperature was 130 °C, and a heating rate of 2 K/min was applied. In order to produce controlled mixtures for phase diagram determination, weighed amounts of racemate and/or enantiomer were mixed and dissolved in acetone, and after evaporation of the solvent the solid was ground to a fine powder. Ten to fifteen milligrams of the respective mixtures were used for DSC experiments.

Solid samples were analyzed throughout by X-ray powder diffraction to identify the solid phases present. An X'Pert Pro diffractometer (PANalytical GmbH, Kassel, Germany) with Cu K$\alpha_1$ radiation was used. Measurements covered a 2$\theta$ range from 3° to 40° with a step size of 0.0167°. Investigations of solvates included the use of NMR to identify possible solvates and exclude the possibility of solvent mediated solvatomorphism.

Solubility measurements were performed by applying a classical isothermal method. A known composition of PPX in dibutylether was prepared (leaving an excess of the solid phase), and the vessels were placed into a temperature-controlled bath and magnetically stirred at a constant temperature (within ±0.01 K) until equilibrium was attained. Subsequently, the liquid and solid phases were separated by filtration and analyzed using HPLC, XRPD, and NMR.

**Racemization Conditions.** A flame-dried 20-mL reaction vessel was charged with (*S*)-PPX and the catalyst; the vessel was closed, evacuated, and flushed with argon three times. The solvent and any additive were subsequently added via syringe. The mixture was stirred at the indicated temperature for a given period of time. After completion of the reaction time, the mixture was cooled to 0 °C for 30−40 min and the PPX crystallized was isolated by filtration. The loss of optical purity was determined by HPLC analysis (AD column, *i*-hexane/ethanol/triethylamine; 85:15:0.1, $t_R(S)$ = 10.33, $t_R(R)$ = 12.65 min). Racemic and enantiopure compounds were used as references.

The multiple use of Shvo catalyst was investigated using a similar procedure, with the exception that racemized PPX was removed after crystallization and fresh (*S*)-PPX was charged prior the next racemization run.

## AUTHOR INFORMATION

### Corresponding Author

*E-mail: seidel-morgenstern@mpi-magdeburg.mpg.de. Telephone: +49-391-6110-401. Fax: +49-391-6110-521.

## ACKNOWLEDGMENTS

This work was funded by the European Union (EU-project "INTENANT, Integrated Synthesis and Purification of Enantiomers"; NMP2-SL-2008-214129).

## REFERENCES

(1) Ekenstam, B.; Egnér, B.; Pettersson, G. *Acta Chem. Scand.* **1957**, *11*, 1183−1190.

(2) See, for instance, the AstraZeneca product monograph for ropivacaine hydrochloride 2004 and references therein.

(3) (a) Adger, B.; Dyer, U.; Hutton, G.; Woods, M. *Tetrahedron. Lett.* **1996**, *37*, 6399−6402. (b) Rinderknecht, H. *Helv. Chim. Acta* **1959**, *42*, 1324. The most cost-efficient and high-yielding routes to racemic **1** judged by overall yield and raw material costs are found in (c) Tullar, B. F.; Bolen, C. H. GB 1166802, 1969 and 1968. (d) Soni R. R.; Koftis, T.; Georgopoulou, I; Karagiannidou, E. PCT Int. Appl. WO/2009/089842, 2009.

(4) Tullar, B. F. *J. Med. Chem.* **1971**, *14*, 891−892. This procedure gave a rather low yield for the diastereomeric salt resolution of 26% (50% maximum). However, internal optimization at former Astra raised the yield to a robust level of 45% by changing solvent and process conditions (not shown).

(5) Commercial availability and pricing data were investigated using the MDL ISIS 2.5 acd commercial catalogue database, available within AstraZeneca, to obtain both lab-scale and bulk-scale prices. Bulk costs were arbitrarily set to 10% of the Aldrich or Acros catalogue prices for each raw material, based upon experience with other compounds. The relative prices for L-lysine/racemic pipecolinic acid/picolinic acid appear to be 1:9:1 if prices from the same manufacturer are used for all three chemicals. With respect to absolute numbers, picolinic acid appears to cost at most 50 USD/kg as assessed from the database. Z-protected L-lysine and enantiopure (*S*)-pipecolinic are both expensive and cost of the order of 500 USD/kg in bulk and according to the database. These cost/price levels may, of course, change depending on demand and other factors.

(6) The most high-yielding procedure was found in Bence, A. K.; Crooks, P. A. *Synth. Commun.* **2002**, *32*, 2075. For an earlier reference where a lower yield was reported, see Baldwin, J. E.; Killin, S. J.; Adlington, R. M.; Spiegel, U. *Tetrahedron* **1988**, *44*, 2633.

(7) A Scifinder search gave 59 reactions describing the synthesis of (*S*)-pipecolinic acid, out of which a few describe methods involving resolution of racemic material.

(8) Reported yields for the amide-coupling to give optically pure **1** are low when starting from enantiopure (*S*)-pipecolinic acid: (a) Tsuchida, T.; Kaneko, K.; Matsumoto, N. European patent EP 1433782; 2005. (b) Pilli, R. A.; Santos, L. S. Brasilian patent BR 2003002250, 2005 (patent written in Portuguese; short abstract in English is available). (c) Rangisetty, J. B.; Pullagurla, M. R.; Muthiah, R. J. J., Jobdevairakkam, C. N., U.S. Patent Appl. 2006/0276654, 2006.
(9) Information about INTENANT is available from the homepage www.intenant.eu.
(10) Kaspereit, M. et al. *Org. Process Res. Dev.* **2012**, 10.1021/op200285v, INTENANT special section this issue.
(11) Kaspereit, M.; Gedicke, K.; Zahn, V.; Mahoney, A. W.; Seidel-Morgenstern, A. *J. Chromatogr. A* **2005**, *1092*, 43−54.
(12) Amanullah, M.; Mazzotti, M. *J. Chromatogr. A* **2006**, *1107*, 36−45.
(13) Gedicke, K.; Kaspereit, M.; Beckmann, W.; Budde, U.; Lorenz, H.; Seidel-Morgenstern, A. *Chem. Eng. Res. Des.* **2007**, *85*, 928−936.
(14) Antos, D.; Seidel-Morgenstern, A. *Chem. Eng. Sci.* **2001**, *56*, 6667−6682.
(15) Antos, D. *Gradient Techniques in Preparative Chromatography − Modelling and Experimental Realization*. PhD Thesis, Oficyna Wydawnicza Politechniki Rzszowskiej, Rzeszow, Poland, 2003.
(16) Chung, S.; Wen, C. *AIChE J.* **1968**, *14*, 857−866.
(17) Guiochon, G.; Shirazi, D. G.; Felinger, A.; Katti, A. M. *Fundamentals of Preparative and Nonlinear Chromatography*; Academic Press: Waltham, U.S.A., 2006.
(18) Felinger, A.; Cavazzini, A.; Guiochon, G. *J. Chromatogr. A.* **2003**, *986*, 207−225.
(19) Bailly, M.; Tondeur, D. *Chem. Eng. Sci.* **1982**, *37*, 1199−1212.
(20) Grill, C. M.; Miller, L. *J. Chromatogr. A* **1998**, *827*, 359−371.
(21) Kaspereit, M.; Sainio, T. *Chem. Eng. Sci.* **2011**, *66*, 5428−5438.
(22) Sainio, T.; Kaspereit, M. *Sep. Purif. Technol.* **2009**, *66*, 9−18.
(23) Jacques, J.; Collet, A.; Wilen, S. H. *Enantiomers, Racemates and Resolutions*; Krieger Publishing Company: Malabar, USA, 1994.
(24) Collins, A. N.; Sheldrake, G. N.; Crosby, J. *Chirality in Industry: The Commercial Manufacture and Applications of Optically Active Compounds*; Wiley & Sons: Chichester, UK, 1992.
(25) Nemák, K.; Ács, M.; Kozma, D.; Fogassy, E. *J. Therm. Anal.* **1997**, *48*, 691−696.
(26) Lorenz, H.; Sheehan, P.; Seidel-Morgenstern, A. *J. Chromatogr. A* **2001**, *908*, 201−214.
(27) Some recent examples of racemization of amines using metal catalysis: (a) Pàmies, O.; Éll, O. A.; Samec, J. S. M.; Hermanns, N.; Bäckvall., J.-E. *Tetrahedron Lett.* **2002**, *43*, 4699−4702. (b) Thalén, L. K.; Zhao, D.; Sortais, J.-B.; Paetzold, J.; Hoben, C.; Bäckvall, J.-E. *Chem. Eur. J.* **2009**, *15*, 3403−3410. (c) Paetzold, J.; Bäckvall, J. E. *J. Am. Chem. Soc.* **2005**, *127*, 17620−17621. (d) Thalén, L. K.; Hermanns, N.; Bäckvall., J.-E. *Tetrahedron Lett.* **2010**, *51*, 6802−6802. (e) Parvulescu, A. N.; Jacobs, P. A.; De Vos, D. E. *Chem.-Eur. J.* **2007**, *13*, 2034−2043. (f) Kim, M.-J.; Kim, W.-H.; Han, K.; Choi, Y.K.; Park. *J. Org. Lett.* **2007**, *9*, 1157−1159. (g) Jerphagnon, T.; Gayet, A. J. A.; Berthiol, F.; Ritleng, V.; Mršić, N.; Meetsma, A.; Pfeffer, M.; Minnaard, A.J.; Feringa, B. L.; de Vries, J. G. *Chem.-Eur. J.* **2009**, *15*, 12780−12790. (h) A useful review article on racemization methodologies in general including metal-mediated racemization: Ebbers, E. J.; Ariaans, G. J. A.; Houbiers, J. P. M.; Bruggink, A.; Zwanenburg, B. *Tetrahedron* **1997**, *53*, 9417−9476.
(28) Dyer, U. C.; Langston, M.; Woods, M. PCT WO 001996022281 A1; 1996.
(29) Internal experiments by Peter Jaksch at AstraZeneca studying racemization of (*R*)-**1** using a stoichiometric ethoxide base at room temperature in EtOH, resulted in clean but slow racemization which was complete in 5 days. Increasing the temperature, of course, resulted in a much faster racemization but also caused significant byproduct formation.